

# SCIENTIFIC PAPERS

---

VI OPORTO BIOMEDICAL SUMMIT



# SCIENTIFIC PAPERS

## INDEX

### Clinical Abstract :

From womb to recovery: navigating the journey of complete d-TGA.....	2
Overlapping classic phenylketonuria and advanced liver disorder: a diagnostic challenge.....	3
Pleural Ultrasound as The Primary Tool for Monitoring Necrotizing Empyema in Infants: A Case Repo.....	4
Robotic Management of Stage 4 Endometriosis: A Case of Diagnostic Discrepancy .....	5

### Research Abstract :

Dissecting PRRXL1 Transcriptional Regulatory Mechanism in Dorsal Spinal Cord Development.....	6
Effects of Clinically Used Contrast Agents on the Actin Cytoskeleton .....	7
Genetic testing previous to kidney transplantation in a cohort of European population: what are we missing? ...	8
Three Vascular Phenotypes in the Spleen Controlled by the Dosage of a Single Transcription Factor .....	9



# Clinical abstract- From womb to recovery: navigating the journey of complete d-TGA



**Student**  
**Wiktorija Lisińska**

## From womb to recovery: navigating the journey of complete d-TGA

Author: Wiktorija Lisińska  
Supervisors : Prof. Iwona Strzelecka PhD, Prof. Maria Respondek-Liberska MD, PhD  
Affiliation: Student Scientific Research Club of Prenatal Cardiology Medical University of Lodz

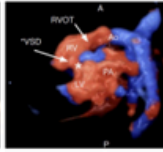
---

### Case history

**Part 1: Prenatal appointment**  
A pregnant **29-year-old patient** at 22 + 6 days of gestation. Her obstetric history included an early pregnancy complication at 6+2 weeks when she was admitted for vaginal bleeding and diagnosed with a **3 cm subchorionic hematoma**. **Second-trimester ultrasound** that raised suspicion of a **congenital heart defect**:  
 → absence of the normal crossover of the great arteries  
 → aorta arising from the right ventricle and the pulmonary artery from the left ventricle  
 → abnormal **three-vessel view and trachea (3VT) view**  
 → abnormal blood flow patterns – visible on color Doppler imaging

**Part 2: Prenatal Cardiology Clinic**  
**Results from fetal echocardiogram:**

- confirmed diagnosis of complete **d-TGA**
- ventricular septal defect (**VSD**)
- outflow congenital heart disease (**CHD**)
- good **atrial communication** (FO index = 33%)
- preserved **pulmonary circulation**.

Prenatal monitoring evaluations at 25, 28, 30, and 34 weeks of gestation. → Stable fetal hemodynamics and expected growth.

**Part 3: Delivery**

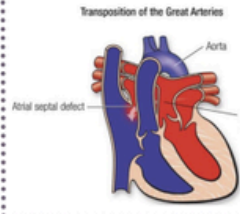
Fetal heart had good atrial communication (FO index=27%)

It was concluded that there was **no immediate need for a Rashkind procedure** (a balloon septostomy) postnatally. → Delivery was performed via **cesarean section**. Neonate was born with a birth weight of **3700 g** with Apgar scores of **5/7/7/7**.

### Introduction

d-TGA is a **congenital** heart disease. It accounts for approximately **8–10%** of all congenital heart defects. Leads to **life-threatening hypoxemia** if untreated.

For the survival of a newborn with a defect, a **connection between the systemic and pulmonary circulation is essential**:  
 → patent foramen ovale  
 → persistent ductus arteriosus  
 → ventricular septal defect  
 → atrial septal defect



### Discussion

**Early prenatal diagnosis of congenital heart defects**, such as complete d-TGA, is crucial for optimizing outcomes.  
 → advancements in prenatal ultrasound screening have significantly improved its detection up to 77%  
 → early pregnancy detection remains challenging due to the normal appearance of the four-chamber heart view and technical limitations in visualizing the great arteries.

The **connections between the systemic and pulmonary blood circulations** in atrial septal defect, patent ductus arteriosus, or ventricular septal defect allow the neonate with TGA to survive until the arterial switch surgery.

d-TGA can present as either a planned or emergent condition:  
 → planned cases: **prostaglandin E1 (PGE1)** is administered to maintain ductal patency until surgery  
 → emergent cases: **immediate postnatal intervention** (balloon atrial septostomy)

### Conclusion

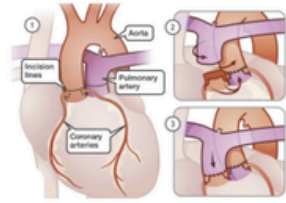
- **Prenatal screening is essential** for the early detection and potential treatment planning of fetal heart defects.
- Although prenatal detection of d-TGA may not change monitoring during pregnancy, it is **essential for timely postnatal intervention** and improves neonatal outcomes.
- The **connections between the systemic and pulmonary** blood circulations allow the neonate with TGA to survive until the arterial switch surgery.

### Part 4: Corrective surgery

**2 weeks of age:** neonate underwent **planned corrective cardiac surgery**

The treatment of choice in surgical management is currently **the Jatene procedure**—anatomical correction, which restores the normal anatomy of the heart.

- is performed in newborns **up to the 3rd week of life**
- is carried out using cardiopulmonary bypass and deep hypothermia.



### Part 5: Postnatal course



- **intensive care** with mechanical ventilation
- **catecholamine** infusion
- teicoplanin and ceftazidime (wound infection)

Follow-up echocardiography confirmed **good myocardial contractility and no pericardial effusion.**

© 2022 Dai A, Ling M, Tang Y, Guo S, Wu H, Huang Q, Deng L, Wang Z, Wu Q. Prenatal transposition of great arteries: diagnosis and management: a Chinese single-center study. *Front Cardiovasc Med.* 2022 May 6;13:1343006. doi: 10.3389/fcvm.2022.1343006. PMID: 36510298 PMCID: PMC9059399

Zhu Q, Deng C, Zhu Q, Tang X, Liu H, Luo F, Wang X, Yu H. Double-transposition of the great arteries in one twin: case reports and literature review. *Transl Pediatr.* 2022 Apr;12(4):605-609. doi: 10.2196/tp.21189. PMID: 35580876 PMCID: PMC9028995

Chen H, Wang B. Four-Dimensional Ultrasound Images of Spatial Relationship of Great Arteries in Fetuses With Transposition of Great Arteries. *J Ultrasound Med.* 2024 Apr;43(4):293-307. doi: 10.1002/ulm.18462. Epub 2024 May 16. PMID: 38732263

El-Anderson BA, Carfagna AJ, Hayes EA, Quaghebur JG, Vicenti JA, Bacha EA. Earlier arterial switch operation improves outcomes and reduces costs for neonates with transposition of the great arteries. *J Am Coll Cardiol.* 2016;68(8):887-7. doi: 10.1016/j.jacc.2016.08.045

© 2022 Kottgen JM, Nishi MK, Fraser CD, Smith DB, Mahanian CA. Revised to Outcome of 323 patients with congenitally corrected transposition of the great arteries. *Pediatr. Cardiol.* 2002;23(2):137-46. doi:10.1007/s00381-002-0307-8

# Clinical abstract- Overlapping classic phenylketonuria and advanced liver disorder: a diagnostic challenge

**Student**  
**Gustavo Matassoli**



## Overlapping classic phenylketonuria and advanced liver disorder: a diagnostic challenge

Machado Inês1,2, Marques Leonor1,2, Matassoli Gustavo1,2, Pereira Sandra1,2 and Magalhães Marina3  
<sup>1</sup>School of Medicine and Biomedical Sciences (ICBAS), University of Porto, Oporto  
<sup>2</sup>These authors contributed equally to this work  
<sup>3</sup>Department of Neurology, Centro Hospitalar Universitário de Santo António, Unidade Local de Saúde de Santo António, 4099-001 Porto, Portugal; diogoteixeira.neurologia@chporto.min-saude.pt (D.P.); marinamagalhaes.neurologia@chporto.min-saude.pt (M.M.)

### Introduction

Phenylketonuria (PKU) is an autosomal recessive metabolic disorder caused by deficiency of phenylalanine hydroxylase, leading to elevated phenylalanine levels and neurotoxicity. Untreated patients may develop intellectual disability, movement disorders and psychiatric symptoms. Since the introduction of neonatal screening programs, late diagnosis has become rare.

Caroli disease, a congenital disorder with intrahepatic bile duct dilatation, may progress to portal hypertension and liver failure, predisposing to hepatic encephalopathy (ammonia-related) and acquired hepatocerebral degeneration (AHD), associated with manganese deposition, both characterized by cognitive impairment and movement disorders.

Figure 3. Metabolism of phenylalanine in individuals with PKU.

### Discussion

In this patient with Caroli disease and advanced liver dysfunction, cognitive decline and movement disorders were initially interpreted as hepatic encephalopathy, supported by elevated ammonia levels, and acquired hepatocerebral degeneration (AHD), suggested by neuroimaging findings. Cranial CT showed bilateral dentate nucleus hypodensity, and brain MRI demonstrated T2/FLAIR hyperintensities involving the pyramidal tracts, centrum semiovale, corpus callosum and subtle basal ganglia changes, patterns described in AHD.

However, serum manganese levels were normal, making classic manganese-related AHD less likely as the sole mechanism. The marked neurological improvement after liver transplantation nevertheless supported the presence of a reversible liver-related neurotoxic component.

The persistence of lifelong neurodevelopmental impairment, together with developmental delay observed in her children, raised suspicion of a coexisting metabolic disorder. Genetic testing ultimately confirmed phenylketonuria (PKU), likely undiagnosed because the patient was born before the implementation of newborn screening. Although the children also presented developmental delay, PKU was not confirmed in them, suggesting possible maternal metabolic exposure during pregnancy.

This case suggests a dual mechanism: a reversible neurological deterioration related to liver dysfunction and a chronic neurodevelopmental impairment due to previously undiagnosed PKU.

### Clinical Case

A 53-year-old woman with known Caroli disease presented in 2019 with progressive neurological deterioration, characterized by psychomotor slowing, mild postural tremor, bilateral dysmetria and dysidiadochokinesia, with preserved gait and postural stability. Cranial CT revealed bilateral hypodensity of the dentate nuclei, raising suspicion of acquired hepatocerebral degeneration (AHD).

Between 2020 and 2021, neurological deterioration progressed with fluctuating dementia, dysarthria, myoclonic tremor, gait instability, generalized chorea and cervical dystonia, accompanied by jaundice, peripheral edema and flapping. Brain MRI findings, together with elevated ammonia levels (76.4 mg/dL), supported the diagnosis of AHD associated with hepatic encephalopathy, despite normal serum manganese levels (8.0 µg/dL).

Figure 2 and 3. MRI findings.

Due to progressive liver disease, the patient underwent liver transplantation in 2021, followed by significant neurological improvement, with reduction of chorea, normalization of coordination and stable gait, with only mild tandem instability.

The presence of lifelong cognitive impairment and similar developmental traits among family members raised suspicion of a hereditary condition. Genetic testing identified homozygous pathogenic variants in the PAH gene, and elevated serum phenylalanine (14 mg/dL) confirmed phenylketonuria. Family screening revealed the patient's brother was also affected, while both children tested negative.

### Conclusions

This case highlights the diagnostic complexity created by the coexistence of neurological conditions, in which liver-related neurotoxicity initially masked an underlying metabolic disorder. A comprehensive evaluation of the patient and family context, particularly the observation of neurodevelopmental impairments in the patient's children, prompted reconsideration beyond the initial explanation of hepatic encephalopathy and acquired hepatocerebral degeneration, ultimately leading to the diagnosis of phenylketonuria (PKU).

It also underscores the importance of neonatal screening, which enables early diagnosis and treatment of PKU, preventing long-term neurological damage and making late diagnoses such as this increasingly rare.

### References

1. Inês M, Leonor M, Leonor J, Sáez M. Acquired hepatocerebral degeneration. *Neuroscience (Paris)*. 2018;212:188-197. doi:10.1016/j.neuro.2018.02.004.
2. Inês M, Sáez M. Recent update on acquired hepatocerebral degeneration. *Transl Clin Organ Transplant*. 2019;15(1):44-53. doi:10.1093/otj/otz014.
3. Inês M, Sáez M. Acquired hepatocerebral degeneration. *Transl Clin Organ Transplant*. 2019;15(1):44-53. doi:10.1093/otj/otz014.
4. Inês M, Sáez M, Sáez M, Sáez M. Acquired hepatocerebral degeneration. *Transl Clin Organ Transplant*. 2019;15(1):44-53. doi:10.1093/otj/otz014.
5. Inês M, Sáez M, Sáez M, Sáez M. Acquired hepatocerebral degeneration. *Transl Clin Organ Transplant*. 2019;15(1):44-53. doi:10.1093/otj/otz014.
6. Inês M, Sáez M, Sáez M, Sáez M. Acquired hepatocerebral degeneration. *Transl Clin Organ Transplant*. 2019;15(1):44-53. doi:10.1093/otj/otz014.
7. Inês M, Sáez M, Sáez M, Sáez M. Acquired hepatocerebral degeneration. *Transl Clin Organ Transplant*. 2019;15(1):44-53. doi:10.1093/otj/otz014.
8. Inês M, Sáez M, Sáez M, Sáez M. Acquired hepatocerebral degeneration. *Transl Clin Organ Transplant*. 2019;15(1):44-53. doi:10.1093/otj/otz014.
9. Inês M, Sáez M, Sáez M, Sáez M. Acquired hepatocerebral degeneration. *Transl Clin Organ Transplant*. 2019;15(1):44-53. doi:10.1093/otj/otz014.
10. Inês M, Sáez M, Sáez M, Sáez M. Acquired hepatocerebral degeneration. *Transl Clin Organ Transplant*. 2019;15(1):44-53. doi:10.1093/otj/otz014.
11. Inês M, Sáez M, Sáez M, Sáez M. Acquired hepatocerebral degeneration. *Transl Clin Organ Transplant*. 2019;15(1):44-53. doi:10.1093/otj/otz014.
12. Inês M, Sáez M, Sáez M, Sáez M. Acquired hepatocerebral degeneration. *Transl Clin Organ Transplant*. 2019;15(1):44-53. doi:10.1093/otj/otz014.

# Clinical abstract- Pleural Ultrasound as The Primary Tool for Monitoring Necrotizing Empyema in Infants: A Case Report



**Student**  
**Elisa-Octavia Velicu**



## Pleural Ultrasound as The Primary Tool for Monitoring Necrotizing Empyema in Infants: A Case Report



Elisa-Octavia Velicu, Diana-Andreea Uşurelu<sup>1,2</sup>, Andrei-Stelian Uşurelu<sup>1</sup>, Alexandru Ulmeanu<sup>1,2</sup>  
Vitalia Andreea-Beatrice<sup>1</sup>

<sup>1</sup>University of Medicine and Pharmacy 'Carol Davila', Bucharest  
<sup>2</sup>Pediatrics Department, Clinical Emergency Hospital for Children 'Grigore Alexandrescu', Bucharest

---

**1 Introduction**

Complicated community-acquired pneumonia with parapneumonic effusion and empyema remains a significant cause of morbidity in young children, particularly in former premature infants.

This case report highlights the value of serial pleural ultrasound in identifying fibrinopurulent loculations and detecting necrotizing complications such as lung abscess, demonstrating its usefulness as a bedside tool for monitoring disease progression and guiding clinical management.

**2 Background**



22-month-old female, ex-premature infant (28+5 weeks, birth weight 1320 g) from a twin pregnancy

NICU hospitalization for 2 months, requiring mechanical ventilation. Received antibiotherapy

Normal psychomotor development. No significant past medical history. Family history non-contributory.

**3 Clinical Case**

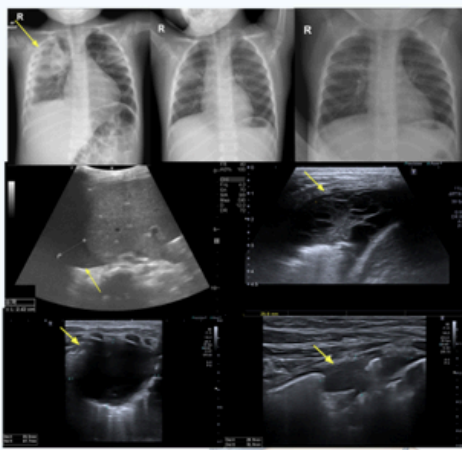
A 22-month-old girl presented with 12 days of high fever (up to 39.5°C) and spasmodic cough, unresponsive to antibiotics, and progressive respiratory distress. At admission, she was febrile (38.5°C) with pallor, upper airway inflammation, and right-sided decreased breath sounds with apical crackles. SpO<sub>2</sub> was 88-90% on room air, improving to 99% with oxygen.

**Key Laboratory Findings at Admission**

<p><b>Hematology</b></p> <ul style="list-style-type: none"> <li>Leukocytosis (with neutrophilia &amp; monocytosis)</li> <li>normochromic normocytic anemia</li> <li>low serum iron (hypoferritinemia)</li> </ul>	<p><b>Inflammatory Markers</b></p> <p>Significantly elevated CRP (15.8 mg/L), Procalcitonin (2.58 ng/mL), Ferritinage (426 ng/mL)</p>
<p><b>Organ Function &amp; Immunology</b></p> <p>Normal renal and hepatic function, normal immunogram, HIV negative</p>	
<p><b>Virology &amp; Microbiology</b></p> <p><b>Positive Pathogens</b></p> <ul style="list-style-type: none"> <li>Co-infection with MRSA and Pseudomonas sp. 2 (detected via respiratory panel)</li> </ul>	<p><b>Bacterial Cultures</b></p> <p>Remained Negative</p>
<p><b>Clinical Course / Follow-up</b></p> <p>Rapid improvement and resolution of the inflammatory syndrome over time (CRP and Procalcitonin dropped to &lt;0.5)</p>	

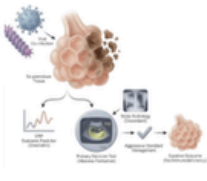
Based on BTS and American Thoracic Society guidelines, and after excluding other pathologies such as tuberculosis, congenital malformations, and aspiration, the patient was diagnosed with stage 2 fibrinopurulent empyema. Considering her ex-premature status and the decline of inflammatory markers, therapy with intravenous meropenem and linezolid, along with oxygen supplementation, was initiated, resulting in favorable clinical evolution.

**4 Imagistic findings**



**5 Discussion**

This case illustrates how viral co-infection in ex-premature infants can accelerate tissue necrosis, and highlights that pleural ultrasound detects abscess formation earlier than static radiography, guiding clinical decision-making.



**6 Conclusion**

This case highlights the decisive role of serial pleural ultrasound in the early detection of fibrinopurulent loculations and necrotizing complications.

Serial PUS enables detection of complications before they become clinically severe

**7 References**

1. Balhoun Lym M et al. BTS guidelines: pleural infection in children. Thorax, 2005.
2. Buonsenso D et al. Parapneumonic empyema in children - scoping review. Ital J Pediatr, 2024.
3. Scauri M et al. EACTS consensus on surgical management of empyema. Eur J Cardiothorac Surg, 2015.
4. Forster J et al. Empiric antibiotic therapy in pediatric empyema (1402 cases). Pediatr Infect Dis J, 2024.
5. Fernández Elviro C et al. Conservative vs surgical management meta-analysis. Chest, 2023.
6. Harris M et al. BTS guidelines: community-acquired pneumonia in children. Thorax, 2011.

# Clinical abstract- Robotic Management of Stage 4 Endometriosis: A Case of Diagnostic Discrepancy

**Student**

**Ferice George Iulian**



## Robotic Management of Stage 4 Endometriosis: A Case of Diagnostic Discrepancy

**Author:** George-Iulian Ferice<sup>1</sup>  
**Co-authors:** Roberta-Andreea Luca<sup>1</sup>, Silvia-Maria Ştirbu<sup>1</sup>, Alexia-Diana Luncan<sup>2</sup>  
**Scientific Coordinator:** Horace Roman M.D. Ph.D. Professor<sup>2,3</sup>

**Affiliations:**  
<sup>1</sup> "Iuliu Hatieganu" University of Medicine and Pharmacy  
<sup>2</sup> Department of Obstetrics and Gynecology, Aarhus University  
<sup>3</sup> Institut Franco-Européen Multidisciplinaire d'Endométriose

---

Introduction

- Endometriosis is a chronic inflammatory disease affecting approximately 10% of reproductive-age women.
- Stage 4 features deep infiltrating lesions impacting the gastrointestinal tract, extra-pelvic structures, and fertility.
- Multidisciplinary, robotic-assisted surgical approach is essential for managing multi-organ infiltration.

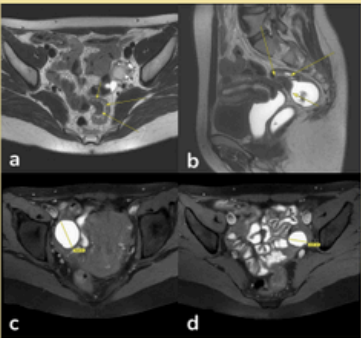


Fig. 1: Endometriosis lesions on MRI.  
a - Ax T2, b - Sag T2 - rectal lesion  
c, d - Ax T1 FS SFOV - ovarian endometrioma

Case Report

- 34-year-old female presenting with dysmenorrhea, daily chronic pelvic pain, positional dyspareunia, and painful defecation, also a 2-year history of primary infertility.
- MRI and transvaginal ultrasound suggested deep infiltrating endometriosis.
- Hysterosalpingography - negative Cotte test on the left side.
- Course of treatment: a three-hour robot-assisted laparoscopy was successfully performed.
- Bilateral ovarian cystectomy - without parenchymal coagulation to preserve ovarian reserve.
- A 9-cm colorectal segment resection using the NOSE technique, extracting the specimen transvaginally.
- A 3-cm white, fibrotic endometriotic lesion on the ileum, causing stenosis and missed on MRI, was resected alongside diaphragmatic lesions.
- Final rASRM score of 78.
- Immediate outcome: restored pelvic anatomy and optimized fertility potential.
- Postoperative continuous dienogest therapy was continued.
- 2-month follow-up: complete resolution of severe symptoms and normal healing of the vaginal vault.

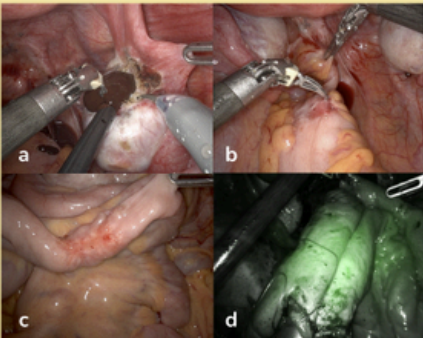


Fig. 2: Intraoperative aspects.  
a - ovarian endometrioma  
b - rectal and Douglas pouch lesions  
c - ileal lesion  
d - side-to-side ileal anastomosis with 60 mm endoGIA stapler and ICG testing

---

Discussion

- Key feature: the significant discrepancy between imaging and surgical findings.
- MRI missed a 3cm ileal nodule and diaphragmatic lesions.
- Robotic assistance was vital for precise nerve-sparing and complex suturing.
- The NOSE technique - minimally invasive extraction, reducing incisional endometriosis risk and enhancing recovery.

References



---

Conclusion

- Endometriosis is a systemic condition that is frequently more extensive than imaging reveals.
- Accurate diagnosis still relies on high clinical suspicion and careful surgical inspection.
- Comprehensive multidisciplinary approach is crucial to reduce the risk of missed lesions.

References



Fig. 3: Resection specimens

# Research abstract- Dissecting PRRXL1 Transcriptional Regulatory Mechanism in Dorsal Spinal Cord Development



**Student**  
**Mafalda Pinto Gomes de Oliveira**

## Dissecting PRRXL1 Transcriptional Regulatory Mechanism in Dorsal Spinal Cord Development

M. Oliveira<sup>1</sup>, H. Saavedra<sup>1</sup>, J. F. Almeida<sup>1</sup>, C. Reguenga<sup>1,2,3</sup>, F. A. Monteiro<sup>1,2,3</sup>  
<sup>1</sup>Departamento de Biomedicina, Faculdade de Medicina, Universidade do Porto, Porto, Portugal, <sup>2</sup>Pain Neurobiology Group, IBMC - Instituto de Biologia Molecular e Celular, Porto, Portugal, <sup>3</sup>IS - Instituto de Investigação e Inovação em Saúde, Porto, Portugal

### INTRODUCTION

During development, precursor neurons differentiate into diverse neuron subtypes by the interplay between extracellular cues and cell-intrinsic genetic programs controlled by combinatorial expression of transcription factors. While the importance of transcription factors in the generation of neuronal diversity is well established, the understanding of molecular mechanisms underlying their function remains limited.

The homeodomain transcription factor PRRXL1 is specifically expressed in developing DRG nociceptors and in glutamatergic neurons of the spinal cord dorsal horn [1,2]. Studies in *Prrxl1* mutant mice revealed that PRRXL1 is required for proper neuronal migration, differentiation, axon guidance, and establishment of the DRG-spinal nociceptive circuitry. To understand the molecular basis of PRRXL1 functions, our research group identified a list of putative PRRXL1 target genes in embryonic DRGs and dorsal spinal cord by combining chromatin immunoprecipitation with gene expression profiling. This experimental strategy was successfully employed on the identification of target genes controlled by the transcription factor TLX3 [3].

### OBJECTIVE

Dissect how PRRXL1 regulates its transcriptional targets at the enhancer level in embryonic dorsal spinal cord.

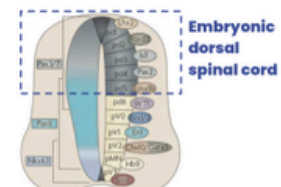
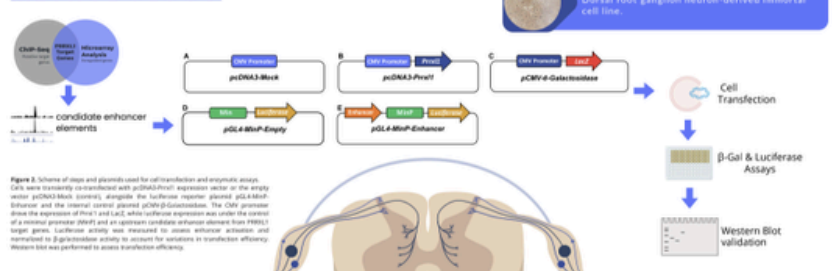


Figure 1. Jankowska, E. (2016). Spinal Interneurons. In: Paine, D., Volkow, N. (eds) Neuroscience in the 21st Century. Springer, New York, NY.

### METHODOLOGY



### RESULTS

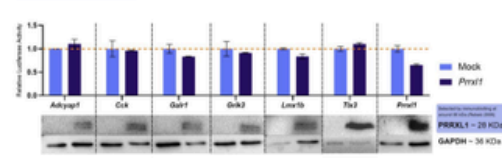


Figure 3. Transcription assays in ND7/23 cells co-transfected with luciferase reporter constructs containing PRRXL1 bound regions (putative enhancers near *Adlyp1*, *Cck*, *Gdf1*, *Grik3*, *Lmx1b*, *Prrxl1*, and *Tlx2* genes) and either an empty (Mock, light blue bars) or a PRRXL1 (dark blue bars) expression construct. Luciferase activity was normalized with β-Galactosidase activity. Data is presented as mean ± SD of technical triplicate assays and represents the fold change of each reporting construct relative to Mock, which is set as 1. Western Blot of the seven enhancers transfected cell lysate.

### CONCLUSIONS

These preliminary data:

- Replicate *Prrxl1* autorepression data [3];
- Indicate an effect of PRRXL1 on enhancers *Adlyp1*, *Grik3* and *Lmx1b* consistent with gene expression studies on knockout mice.

The effects on enhancers *Cck*, *Gdf1*, and *Tlx2* were not consistent with *in vivo* studies, indicating either an effect on a different enhancer, an indirect PRRXL1 regulation, or a lack of cellular context.

### REFERENCES

- [1] Bebevs, S., Reguenga, C., Obeiro, J., Pereira, C., Lopes, C., and Lima, D. (2007). BRG1 immunohistochemical expression during embryonic development in the mouse. *Dev Dyn* 236, 2653-2660.
- [2] Saito, T., Greenwood, A., Sun, Q., and Anderson, DJ. (1995). Identification by differential RT-PCR of a novel paired homeodomain protein specifically expressed in sensory neurons and a subset of their CNS targets. *Mol Cell Neurosci* 6, 280-290.
- [3] Monteiro, C. B., Costa, M. F., Reguenga, C., Lima, D., Castro, D. S., & Monteiro, F. A. (2014). Paired related homeobox protein Bix 1 (*Prrxl1*) controls its own expression by a transcriptional autorepression mechanism. *PLoS One* 9(8):e107340.

# Research abstract- Effects of Clinically Used Contrast Agents on the Actin Cytoskeleton

Student

Zétény Előd Csonka



## Effects of clinically used contrast agent on the actin cytoskeleton

**Zétény Előd Csonka and Zoltán Ujfalusi**

Department of Biophysics, Medical School, University of Pécs; Pécs, Sziget str. 12, H-7624, Hungary

### Introduction, Objectives & Methods

Actin is a fundamental, highly conserved protein in eukaryotic cells that plays a key role in cell motility, division, and vesicle transport. It is evident that the proper functioning of this molecule is essential for cell survival, and any damage can lead to cell death.

Iodine-based (CT) and gadolinium-based (MRI) contrast agents, widely used in medical imaging, improve diagnostic resolution. However, they can cause nephrotoxicity as a side effect, and the underlying cellular mechanisms are not fully understood.

The aim of our study was to investigate whether these contrast agents affect actin's functional dynamics and structure. We examined the effects of Iomeprol (Iomeprol), Visipaque (iodixanol), Xenetix (Iobitridol), and the gadolinium-based Dotarem (gadoterate) and Primovist (disodium gadovetate) at various concentrations. Our experiments employed co-sedimentation assays (to evaluate post-polymerization dynamics), differential scanning calorimetry (DSC, for protein stability), and fluorescence spectroscopy (to determine the critical concentration). According to the literature, different cell types are capable of taking up contrast agents, allowing intracellular interactions between the two substances. Such concentrations can be particularly significant in kidney cells and, for example, in the heart during cardiac catheterization.

**Figure 1**  
Three dimensional structural models of monomeric and filamentous skeletal actin isoform based on the pdb files 2ZWH and 1MVW indicating the position of the „monomer” in the filament and its four subdomains.

### Results

**Figure 2**  
Co-sedimentation assays were performed to assess the G/F-actin ratio after dynamic equilibrium had been established. For all three iodinated contrast agents, increasing concentrations led to a progressive rise in the proportion of free G-actin compared to control. These results indicate a concentration-dependent effect and suggest that the agents promote actin depolymerization.

**Figure 3**  
In the case of the paramagnetic Dotarem, a distinct effect from the iodinated agents was observed. Here, increasing concentrations led to a decrease in the proportion of free G-actin, indicating a stabilizing effect on F-actin and inhibition of depolymerization. This stabilizing effect was also concentration-dependent. (Statistics: Unpaired t-test, \* if  $p < 0.05$ , \*\* if  $p < 0.001$ )

**Figure 4**  
DSC curves of 46  $\mu$ M F-actin in the presence of different concentrations of Visipaque. The treated samples show a decrease in the melting temperature ( $T_m$ ) of actin, indicating that Visipaque binds to the protein and destabilizes its structure in a concentration-dependent manner.

**Figure 5**  
Similar to Visipaque, Iomeprol also reduces the melting temperature ( $T_m$ ) of F-actin. Notably, this destabilizing effect is much more pronounced for filamentous (F-) actin than for monomeric (G-) actin, indicating a stronger impact on the polymerized form.

**Figure 6**  
The critical concentration was determined using pyrene-labeled actin. The special feature of pyrene-labeled actin is that when only G-actin is present in the system (i.e., below the critical concentration), the fluorescence emission intensity detected by the fluorimeter remains constant at a lower level. Once polymerization begins, the emission intensity increases. The intersection point of straight lines fitted to these two phases was used to determine the critical concentration. All three iodinated contrast agents caused a significant increase in the critical concentration compared to the control. Xenetix and Visipaque showed noticeable effects even at lower concentrations and reached a higher maximal effect than Iomeprol. (Statistics: Unpaired t-test, \* if  $p < 0.05$ , \*\* if  $p < 0.001$ )

**Figure 7**  
Both paramagnetic contrast agents significantly reduced the critical concentration even at extremely low concentrations. Increasing the amount of contrast agent did not result in any further meaningful decrease; instead, a plateau phase was observed. (Statistics: Unpaired t-test, \* if  $p < 0.05$ , \*\* if  $p < 0.001$ )

### References

- Zoltán Ujfalusi, Elek Tólek, Miklós Nyitrai, Péter Bognár, Tamás Roskás, Gabriella Hild, László Tré, Gábor Hild. (2022) *Thermochimica Acta* [150], 179185
- Frankle, R. P., Scharnweber, T., Fuhrmann, R., Kruger, A., Wenzel, F., Mrowietz, C., and Jung, F. (2013) *Clin Hemorheol Microcirc* 55(4), 481-490
- Frankle, R. P., Scharnweber, T., Fuhrmann, R., Mrowietz, C., and Jung, F. (2013) *Clin Hemorheol Microcirc* 54(3), 273-285
- Frankle, R. P., Scharnweber, T., Fuhrmann, R., Mrowietz, C., Wenzel, F., Kruger, A., and Jung, F. (2014) *Clin Hemorheol Microcirc* 58(2), 49-63
- Giorgi, M., Ammerman, J., Briffaux, J. P., Fretellier, N., Corot, C., and Bourinnet, P. (2015) *Regul Toxicol Pharmacol* 73(3), 960-970

### Acknowledgements

Janosne Brunner for actin preparation.

In summary, our measurements confirm that a real interaction occurred between the two materials, as the contrast agent affected several important properties of actin. Regardless of its “direction,” this interaction is detrimental to cellular function because it interferes with finely tuned dynamics. As a result, the cell may die, suggesting that this interaction may represent a possible mechanism in the development of contrast-induced nephropathy.

# Research abstract- Genetic testing previous to kidney transplantation in a cohort of European population: what are we missing?

Student

Leonor dos Santos Caetano Dias



**Leonor dos Santos Caetano Dias**  
Oporto Biomedical Summit

**GENETIC TESTING PREVIOUS TO KIDNEY TRANSPLANTATION IN A COHORT OF EUROPEAN POPULATION:  
What are we missing?**

**Background**

CKD affects approximately **10% of the adult population** standing a **major public health challenge**. Genetic factors contribute substantially to CKD etiology, with **monogenic causes identified in up to 20%**.

**Methodology**

- **Retrospective single-center study** including **278 adult patients** referred for **kidney transplant evaluation** between January and June 2022.
- **Eligibility for genetic testing** was assessed according to **KDIGO-based clinical criteria**
- **Collected variables** included CKD etiology, age at kidney replacement therapy initiation, family history, extra-renal manifestations, kidney biopsy data, and previous genetic testing

**Objectives**

1. Assess how **many patients referred for kidney transplant evaluation fulfilled KDIGO-based criteria** for genetic testing. We hypothesize that a considerable proportion of cases with uncertain diagnosis fulfill KDIGO guidelines and remain under-evaluated.
2. **Compare clinical characteristics** between candidates for first and subsequent kidney transplantation

**Results**

- **Unknown etiology:** 29.1% (n=81)
- **Eligible for genetic testing:** 44.6% (n=124)
- **Actually tested:** 10.1% (n=28)
- 16 of 28 patients had **positive hereditary/monogenic diagnosis**

Our main finding is a **clear implementation gap**: although nearly half of the cohort fulfilled criteria for genetic testing, only a small minority had been tested

- **Biopsy status unavailable** in 56.8%
- **Family history missing** in 56.8%.

This suggests that **important diagnostic opportunities may be missed** during routine pre-transplant work-up

- **Re-transplant candidates were more likely to fulfill criteria for genetic testing** than first-transplant candidates (66.8% vs 38.8%). Median age was 55 versus 59 years, and median age at KRT initiation was 35 versus 55 years

**Discussion**

- These findings highlight the **pre-transplant pathway as an important opportunity for structured etiological assessment**
- Greater integration of **genetic testing into transplant evaluation may improve diagnostic accuracy** and support more personalized care
- **Re-transplant candidates may represent a particularly relevant target group for systematic genetic assessment**

**Conclusion**

**High diagnostic uncertainty in transplant candidates**  
Patients evaluated for **second kidney transplantation were more frequently eligible for genetic testing**, making etiologic clarification essential to assess recurrence risk and ensure safe living donor selection, particularly among biologically related donors.

**Large gap between indication and implementation of genetic testing**  
Given the high proportion of patients meeting criteria for genetic testing in this Portuguese cohort, **integrating genetic counselling within nephrology transplant teams and implementing structured family history assessment** may improve diagnosis, transplant planning

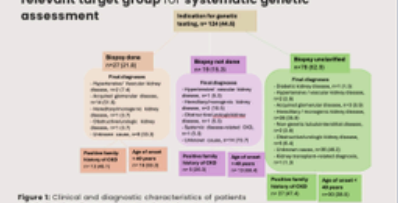


**Figure 1:** Clinical and diagnostic characteristics of patients with indications for genetic testing in study cohort



# Research abstract- Three Vascular Phenotypes in the Spleen Controlled by the Dosage of a Single Transcription Factor

**Student**  
**Kata Váradi**



UNIVERSITY OF PÉCS  
1327

NEMZETI TUDÓS AKADÉMIA  
NATIONAL SCIENTISTS ACADEMY

## Three Vascular Phenotypes in the Spleen Controlled by the Dosage of a Single Transcription Factor

Kata Váradi<sup>1,2</sup>, Diána Heidt<sup>1</sup>, Gergely Berta<sup>1</sup>, Péter Balogh<sup>1</sup>

**AFFILIATIONS**

<sup>1</sup>Department of Immunology and Biotechnology, Medical School, University of Pécs, Pécs, Hungary

<sup>2</sup>Department of Medical Biology, Medical School, University of Pécs, Pécs, Hungary

---

### 01. Introduction

The spleen is a specialized secondary lymphoid organ that filters blood-borne antigens and coordinates adaptive immune responses through a highly organized stromal and vascular microenvironment. Endothelial differentiation within this system is tightly regulated by transcription factors, including the homeodomain protein Nkx2-3. Nkx2-3 plays a key role in establishing splenic vascular identity and regulating the expression of the vascular addressin MAdCAM-1, which mediates lymphocyte homing. While complete loss of Nkx2-3 disrupts splenic vascular architecture, we identified previously undescribed ectopic MAdCAM-1<sup>hi</sup> capillary-like vessels in the red pulp of Nkx2-3 heterozygous mice, suggesting a gene-dose-dependent role of Nkx2-3 in endothelial specification.

### 02. Objective

This study aimed to investigate how altered dosage of Nkx2-3 affects splenic vascular organization.

- Comparing the vascular phenotype of Nkx2-3 heterozygous and knockout mice.
- Characterizing ectopic endothelial structures emerging in the red pulp of Nkx2-3 heterozygous mice.
- Defining the molecular identity of these vessels, including expression of MAdCAM-1 and endothelial adhesion molecules.
- Evaluating the potential role of these ectopic vessels in lymphocyte homing.

---

### 03.A Methods - Nkx2-3<sup>-/-</sup> (KO) mice

**EXPERIMENTAL ANIMALS**

Nkx2-3<sup>-/-</sup> mice were generated by homologous recombination between loxP sites flanking the Nkx2-3 gene in ES cells. Mice were genotyped by PCR. Blood was collected by cardiac puncture. All procedures followed were approved by the Institutional Animal Care and Use Committee (IACUC) of the University of Pécs.

**SINGLE IMMUNOFLOUORESCENT STAINING**

Spleen sections were stained with anti-Nkx2-3 (1:1000), anti-MAdCAM-1 (1:1000), anti-CD31 (1:1000), anti-CD45 (1:1000), anti-CD117 (1:1000), anti-CD133 (1:1000), anti-CD135 (1:1000), anti-CD138 (1:1000), anti-CD146 (1:1000), anti-CD147 (1:1000), anti-CD148 (1:1000), anti-CD149 (1:1000), anti-CD151 (1:1000), anti-CD152 (1:1000), anti-CD153 (1:1000), anti-CD154 (1:1000), anti-CD155 (1:1000), anti-CD156 (1:1000), anti-CD157 (1:1000), anti-CD158 (1:1000), anti-CD159 (1:1000), anti-CD160 (1:1000), anti-CD161 (1:1000), anti-CD162 (1:1000), anti-CD163 (1:1000), anti-CD164 (1:1000), anti-CD165 (1:1000), anti-CD166 (1:1000), anti-CD167 (1:1000), anti-CD168 (1:1000), anti-CD169 (1:1000), anti-CD170 (1:1000), anti-CD171 (1:1000), anti-CD172 (1:1000), anti-CD173 (1:1000), anti-CD174 (1:1000), anti-CD175 (1:1000), anti-CD176 (1:1000), anti-CD177 (1:1000), anti-CD178 (1:1000), anti-CD179 (1:1000), anti-CD180 (1:1000), anti-CD181 (1:1000), anti-CD182 (1:1000), anti-CD183 (1:1000), anti-CD184 (1:1000), anti-CD185 (1:1000), anti-CD186 (1:1000), anti-CD187 (1:1000), anti-CD188 (1:1000), anti-CD189 (1:1000), anti-CD190 (1:1000), anti-CD191 (1:1000), anti-CD192 (1:1000), anti-CD193 (1:1000), anti-CD194 (1:1000), anti-CD195 (1:1000), anti-CD196 (1:1000), anti-CD197 (1:1000), anti-CD198 (1:1000), anti-CD199 (1:1000), anti-CD200 (1:1000), anti-CD201 (1:1000), anti-CD202 (1:1000), anti-CD203 (1:1000), anti-CD204 (1:1000), anti-CD205 (1:1000), anti-CD206 (1:1000), anti-CD207 (1:1000), anti-CD208 (1:1000), anti-CD209 (1:1000), anti-CD210 (1:1000), anti-CD211 (1:1000), anti-CD212 (1:1000), anti-CD213 (1:1000), anti-CD214 (1:1000), anti-CD215 (1:1000), anti-CD216 (1:1000), anti-CD217 (1:1000), anti-CD218 (1:1000), anti-CD219 (1:1000), anti-CD220 (1:1000), anti-CD221 (1:1000), anti-CD222 (1:1000), anti-CD223 (1:1000), anti-CD224 (1:1000), anti-CD225 (1:1000), anti-CD226 (1:1000), anti-CD227 (1:1000), anti-CD228 (1:1000), anti-CD229 (1:1000), anti-CD230 (1:1000), anti-CD231 (1:1000), anti-CD232 (1:1000), anti-CD233 (1:1000), anti-CD234 (1:1000), anti-CD235 (1:1000), anti-CD236 (1:1000), anti-CD237 (1:1000), anti-CD238 (1:1000), anti-CD239 (1:1000), anti-CD240 (1:1000), anti-CD241 (1:1000), anti-CD242 (1:1000), anti-CD243 (1:1000), anti-CD244 (1:1000), anti-CD245 (1:1000), anti-CD246 (1:1000), anti-CD247 (1:1000), anti-CD248 (1:1000), anti-CD249 (1:1000), anti-CD250 (1:1000), anti-CD251 (1:1000), anti-CD252 (1:1000), anti-CD253 (1:1000), anti-CD254 (1:1000), anti-CD255 (1:1000), anti-CD256 (1:1000), anti-CD257 (1:1000), anti-CD258 (1:1000), anti-CD259 (1:1000), anti-CD260 (1:1000), anti-CD261 (1:1000), anti-CD262 (1:1000), anti-CD263 (1:1000), anti-CD264 (1:1000), anti-CD265 (1:1000), anti-CD266 (1:1000), anti-CD267 (1:1000), anti-CD268 (1:1000), anti-CD269 (1:1000), anti-CD270 (1:1000), anti-CD271 (1:1000), anti-CD272 (1:1000), anti-CD273 (1:1000), anti-CD274 (1:1000), anti-CD275 (1:1000), anti-CD276 (1:1000), anti-CD277 (1:1000), anti-CD278 (1:1000), anti-CD279 (1:1000), anti-CD280 (1:1000), anti-CD281 (1:1000), anti-CD282 (1:1000), anti-CD283 (1:1000), anti-CD284 (1:1000), anti-CD285 (1:1000), anti-CD286 (1:1000), anti-CD287 (1:1000), anti-CD288 (1:1000), anti-CD289 (1:1000), anti-CD290 (1:1000), anti-CD291 (1:1000), anti-CD292 (1:1000), anti-CD293 (1:1000), anti-CD294 (1:1000), anti-CD295 (1:1000), anti-CD296 (1:1000), anti-CD297 (1:1000), anti-CD298 (1:1000), anti-CD299 (1:1000), anti-CD300 (1:1000), anti-CD301 (1:1000), anti-CD302 (1:1000), anti-CD303 (1:1000), anti-CD304 (1:1000), anti-CD305 (1:1000), anti-CD306 (1:1000), anti-CD307 (1:1000), anti-CD308 (1:1000), anti-CD309 (1:1000), anti-CD310 (1:1000), anti-CD311 (1:1000), anti-CD312 (1:1000), anti-CD313 (1:1000), anti-CD314 (1:1000), anti-CD315 (1:1000), anti-CD316 (1:1000), anti-CD317 (1:1000), anti-CD318 (1:1000), anti-CD319 (1:1000), anti-CD320 (1:1000), anti-CD321 (1:1000), anti-CD322 (1:1000), anti-CD323 (1:1000), anti-CD324 (1:1000), anti-CD325 (1:1000), anti-CD326 (1:1000), anti-CD327 (1:1000), anti-CD328 (1:1000), anti-CD329 (1:1000), anti-CD330 (1:1000), anti-CD331 (1:1000), anti-CD332 (1:1000), anti-CD333 (1:1000), anti-CD334 (1:1000), anti-CD335 (1:1000), anti-CD336 (1:1000), anti-CD337 (1:1000), anti-CD338 (1:1000), anti-CD339 (1:1000), anti-CD340 (1:1000), anti-CD341 (1:1000), anti-CD342 (1:1000), anti-CD343 (1:1000), anti-CD344 (1:1000), anti-CD345 (1:1000), anti-CD346 (1:1000), anti-CD347 (1:1000), anti-CD348 (1:1000), anti-CD349 (1:1000), anti-CD350 (1:1000), anti-CD351 (1:1000), anti-CD352 (1:1000), anti-CD353 (1:1000), anti-CD354 (1:1000), anti-CD355 (1:1000), anti-CD356 (1:1000), anti-CD357 (1:1000), anti-CD358 (1:1000), anti-CD359 (1:1000), anti-CD360 (1:1000), anti-CD361 (1:1000), anti-CD362 (1:1000), anti-CD363 (1:1000), anti-CD364 (1:1000), anti-CD365 (1:1000), anti-CD366 (1:1000), anti-CD367 (1:1000), anti-CD368 (1:1000), anti-CD369 (1:1000), anti-CD370 (1:1000), anti-CD371 (1:1000), anti-CD372 (1:1000), anti-CD373 (1:1000), anti-CD374 (1:1000), anti-CD375 (1:1000), anti-CD376 (1:1000), anti-CD377 (1:1000), anti-CD378 (1:1000), anti-CD379 (1:1000), anti-CD380 (1:1000), anti-CD381 (1:1000), anti-CD382 (1:1000), anti-CD383 (1:1000), anti-CD384 (1:1000), anti-CD385 (1:1000), anti-CD386 (1:1000), anti-CD387 (1:1000), anti-CD388 (1:1000), anti-CD389 (1:1000), anti-CD390 (1:1000), anti-CD391 (1:1000), anti-CD392 (1:1000), anti-CD393 (1:1000), anti-CD394 (1:1000), anti-CD395 (1:1000), anti-CD396 (1:1000), anti-CD397 (1:1000), anti-CD398 (1:1000), anti-CD399 (1:1000), anti-CD400 (1:1000), anti-CD401 (1:1000), anti-CD402 (1:1000), anti-CD403 (1:1000), anti-CD404 (1:1000), anti-CD405 (1:1000), anti-CD406 (1:1000), anti-CD407 (1:1000), anti-CD408 (1:1000), anti-CD409 (1:1000), anti-CD410 (1:1000), anti-CD411 (1:1000), anti-CD412 (1:1000), anti-CD413 (1:1000), anti-CD414 (1:1000), anti-CD415 (1:1000), anti-CD416 (1:1000), anti-CD417 (1:1000), anti-CD418 (1:1000), anti-CD419 (1:1000), anti-CD420 (1:1000), anti-CD421 (1:1000), anti-CD422 (1:1000), anti-CD423 (1:1000), anti-CD424 (1:1000), anti-CD425 (1:1000), anti-CD426 (1:1000), anti-CD427 (1:1000), anti-CD428 (1:1000), anti-CD429 (1:1000), anti-CD430 (1:1000), anti-CD431 (1:1000), anti-CD432 (1:1000), anti-CD433 (1:1000), anti-CD434 (1:1000), anti-CD435 (1:1000), anti-CD436 (1:1000), anti-CD437 (1:1000), anti-CD438 (1:1000), anti-CD439 (1:1000), anti-CD440 (1:1000), anti-CD441 (1:1000), anti-CD442 (1:1000), anti-CD443 (1:1000), anti-CD444 (1:1000), anti-CD445 (1:1000), anti-CD446 (1:1000), anti-CD447 (1:1000), anti-CD448 (1:1000), anti-CD449 (1:1000), anti-CD450 (1:1000), anti-CD451 (1:1000), anti-CD452 (1:1000), anti-CD453 (1:1000), anti-CD454 (1:1000), anti-CD455 (1:1000), anti-CD456 (1:1000), anti-CD457 (1:1000), anti-CD458 (1:1000), anti-CD459 (1:1000), anti-CD460 (1:1000), anti-CD461 (1:1000), anti-CD462 (1:1000), anti-CD463 (1:1000), anti-CD464 (1:1000), anti-CD465 (1:1000), anti-CD466 (1:1000), anti-CD467 (1:1000), anti-CD468 (1:1000), anti-CD469 (1:1000), anti-CD470 (1:1000), anti-CD471 (1:1000), anti-CD472 (1:1000), anti-CD473 (1:1000), anti-CD474 (1:1000), anti-CD475 (1:1000), anti-CD476 (1:1000), anti-CD477 (1:1000), anti-CD478 (1:1000), anti-CD479 (1:1000), anti-CD480 (1:1000), anti-CD481 (1:1000), anti-CD482 (1:1000), anti-CD483 (1:1000), anti-CD484 (1:1000), anti-CD485 (1:1000), anti-CD486 (1:1000), anti-CD487 (1:1000), anti-CD488 (1:1000), anti-CD489 (1:1000), anti-CD490 (1:1000), anti-CD491 (1:1000), anti-CD492 (1:1000), anti-CD493 (1:1000), anti-CD494 (1:1000), anti-CD495 (1:1000), anti-CD496 (1:1000), anti-CD497 (1:1000), anti-CD498 (1:1000), anti-CD499 (1:1000), anti-CD500 (1:1000), anti-CD501 (1:1000), anti-CD502 (1:1000), anti-CD503 (1:1000), anti-CD504 (1:1000), anti-CD505 (1:1000), anti-CD506 (1:1000), anti-CD507 (1:1000), anti-CD508 (1:1000), anti-CD509 (1:1000), anti-CD510 (1:1000), anti-CD511 (1:1000), anti-CD512 (1:1000), anti-CD513 (1:1000), anti-CD514 (1:1000), anti-CD515 (1:1000), anti-CD516 (1:1000), anti-CD517 (1:1000), anti-CD518 (1:1000), anti-CD519 (1:1000), anti-CD520 (1:1000), anti-CD521 (1:1000), anti-CD522 (1:1000), anti-CD523 (1:1000), anti-CD524 (1:1000), anti-CD525 (1:1000), anti-CD526 (1:1000), anti-CD527 (1:1000), anti-CD528 (1:1000), anti-CD529 (1:1000), anti-CD530 (1:1000), anti-CD531 (1:1000), anti-CD532 (1:1000), anti-CD533 (1:1000), anti-CD534 (1:1000), anti-CD535 (1:1000), anti-CD536 (1:1000), anti-CD537 (1:1000), anti-CD538 (1:1000), anti-CD539 (1:1000), anti-CD540 (1:1000), anti-CD541 (1:1000), anti-CD542 (1:1000), anti-CD543 (1:1000), anti-CD544 (1:1000), anti-CD545 (1:1000), anti-CD546 (1:1000), anti-CD547 (1:1000), anti-CD548 (1:1000), anti-CD549 (1:1000), anti-CD550 (1:1000), anti-CD551 (1:1000), anti-CD552 (1:1000), anti-CD553 (1:1000), anti-CD554 (1:1000), anti-CD555 (1:1000), anti-CD556 (1:1000), anti-CD557 (1:1000), anti-CD558 (1:1000), anti-CD559 (1:1000), anti-CD560 (1:1000), anti-CD561 (1:1000), anti-CD562 (1:1000), anti-CD563 (1:1000), anti-CD564 (1:1000), anti-CD565 (1:1000), anti-CD566 (1:1000), anti-CD567 (1:1000), anti-CD568 (1:1000), anti-CD569 (1:1000), anti-CD570 (1:1000), anti-CD571 (1:1000), anti-CD572 (1:1000), anti-CD573 (1:1000), anti-CD574 (1:1000), anti-CD575 (1:1000), anti-CD576 (1:1000), anti-CD577 (1:1000), anti-CD578 (1:1000), anti-CD579 (1:1000), anti-CD580 (1:1000), anti-CD581 (1:1000), anti-CD582 (1:1000), anti-CD583 (1:1000), anti-CD584 (1:1000), anti-CD585 (1:1000), anti-CD586 (1:1000), anti-CD587 (1:1000), anti-CD588 (1:1000), anti-CD589 (1:1000), anti-CD590 (1:1000), anti-CD591 (1:1000), anti-CD592 (1:1000), anti-CD593 (1:1000), anti-CD594 (1:1000), anti-CD595 (1:1000), anti-CD596 (1:1000), anti-CD597 (1:1000), anti-CD598 (1:1000), anti-CD599 (1:1000), anti-CD600 (1:1000), anti-CD601 (1:1000), anti-CD602 (1:1000), anti-CD603 (1:1000), anti-CD604 (1:1000), anti-CD605 (1:1000), anti-CD606 (1:1000), anti-CD607 (1:1000), anti-CD608 (1:1000), anti-CD609 (1:1000), anti-CD610 (1:1000), anti-CD611 (1:1000), anti-CD612 (1:1000), anti-CD613 (1:1000), anti-CD614 (1:1000), anti-CD615 (1:1000), anti-CD616 (1:1000), anti-CD617 (1:1000), anti-CD618 (1:1000), anti-CD619 (1:1000), anti-CD620 (1:1000), anti-CD621 (1:1000), anti-CD622 (1:1000), anti-CD623 (1:1000), anti-CD624 (1:1000), anti-CD625 (1:1000), anti-CD626 (1:1000), anti-CD627 (1:1000), anti-CD628 (1:1000), anti-CD629 (1:1000), anti-CD630 (1:1000), anti-CD631 (1:1000), anti-CD632 (1:1000), anti-CD633 (1:1000), anti-CD634 (1:1000), anti-CD635 (1:1000), anti-CD636 (1:1000), anti-CD637 (1:1000), anti-CD638 (1:1000), anti-CD639 (1:1000), anti-CD640 (1:1000), anti-CD641 (1:1000), anti-CD642 (1:1000), anti-CD643 (1:1000), anti-CD644 (1:1000), anti-CD645 (1:1000), anti-CD646 (1:1000), anti-CD647 (1:1000), anti-CD648 (1:1000), anti-CD649 (1:1000), anti-CD650 (1:1000), anti-CD651 (1:1000), anti-CD652 (1:1000), anti-CD653 (1:1000), anti-CD654 (1:1000), anti-CD655 (1:1000), anti-CD656 (1:1000), anti-CD657 (1:1000), anti-CD658 (1:1000), anti-CD659 (1:1000), anti-CD660 (1:1000), anti-CD661 (1:1000), anti-CD662 (1:1000), anti-CD663 (1:1000), anti-CD664 (1:1000), anti-CD665 (1:1000), anti-CD666 (1:1000), anti-CD667 (1:1000), anti-CD668 (1:1000), anti-CD669 (1:1000), anti-CD670 (1:1000), anti-CD671 (1:1000), anti-CD672 (1:1000), anti-CD673 (1:1000), anti-CD674 (1:1000), anti-CD675 (1:1000), anti-CD676 (1:1000), anti-CD677 (1:1000), anti-CD678 (1:1000), anti-CD679 (1:1000), anti-CD680 (1:1000), anti-CD681 (1:1000), anti-CD682 (1:1000), anti-CD683 (1:1000), anti-CD684 (1:1000), anti-CD685 (1:1000), anti-CD686 (1:1000), anti-CD687 (1:1000), anti-CD688 (1:1000), anti-CD689 (1:1000), anti-CD690 (1:1000), anti-CD691 (1:1000), anti-CD692 (1:1000), anti-CD693 (1:1000), anti-CD694 (1:1000), anti-CD695 (1:1000), anti-CD696 (1:1000), anti-CD697 (1:1000), anti-CD698 (1:1000), anti-CD699 (1:1000), anti-CD700 (1:1000), anti-CD701 (1:1000), anti-CD702 (1:1000), anti-CD703 (1:1000), anti-CD704 (1:1000), anti-CD705 (1:1000), anti-CD706 (1:1000), anti-CD707 (1:1000), anti-CD708 (1:1000), anti-CD709 (1:1000), anti-CD710 (1:1000), anti-CD711 (1:1000), anti-CD712 (1:1000), anti-CD713 (1:1000), anti-CD714 (1:1000), anti-CD715 (1:1000), anti-CD716 (1:1000), anti-CD717 (1:1000), anti-CD718 (1:1000), anti-CD719 (1:1000), anti-CD720 (1:1000), anti-CD721 (1:1000), anti-CD722 (1:1000), anti-CD723 (1:1000), anti-CD724 (1:1000), anti-CD725 (1:1000), anti-CD726 (1:1000), anti-CD727 (1:1000), anti-CD728 (1:1000), anti-CD729 (1:1000), anti-CD730 (1:1000), anti-CD731 (1:1000), anti-CD732 (1:1000), anti-CD733 (1:1000), anti-CD734 (1:1000), anti-CD735 (1:1000), anti-CD736 (1:1000), anti-CD737 (1:1000), anti-CD738 (1:1000), anti-CD739 (1:1000), anti-CD740 (1:1000), anti-CD741 (1:1000), anti-CD742 (1:1000), anti-CD743 (1:1000), anti-CD744 (1:1000), anti-CD745 (1:1000), anti-CD746 (1:1000), anti-CD747 (1:1000), anti-CD748 (1:1000), anti-CD749 (1:1000), anti-CD750 (1:1000), anti-CD751 (1:1000), anti-CD752 (1:1000), anti-CD753 (1:1000), anti-CD754 (1:1000), anti-CD755 (1:1000), anti-CD756 (1:1000), anti-CD757 (1:1000), anti-CD758 (1:1000), anti-CD759 (1:1000), anti-CD760 (1:1000), anti-CD761 (1:1000), anti-CD762 (1:1000), anti-CD763 (1:1000), anti-CD764 (1:1000), anti-CD765 (1:1000), anti-CD766 (1:1000), anti-CD767 (1:1000), anti-CD768 (1:1000), anti-CD769 (1:1000), anti-CD770 (1:1000), anti-CD771 (1:1000), anti-CD772 (1:1000), anti-CD773 (1:1000), anti-CD774 (1:1000), anti-CD775 (1:1000), anti-CD776 (1:1000), anti-CD777 (1:1000), anti-CD778 (1:1000), anti-CD779 (1:1000), anti-CD780 (1:1000), anti-CD781 (1:1000), anti-CD782 (1:1000), anti-CD783 (1:1000), anti-CD784 (1:1000), anti-CD785 (1:1000), anti-CD786 (1:1000), anti-CD787 (1:1000), anti-CD788 (1:1000), anti-CD789 (1:1000), anti-CD790 (1:1000), anti-CD791 (1:1000), anti-CD792 (1:1000), anti-CD793 (1:1000), anti-CD794 (1:1000), anti-CD795 (1:1000), anti-CD796 (1:1000), anti-CD797 (1:1000), anti-CD798 (1:1000), anti-CD799 (1:1000), anti-CD800 (1:1000), anti-CD801 (1:1000), anti-CD802 (1:1000), anti-CD803 (1:1000), anti-CD804 (1:1000), anti-CD805 (1:1000), anti-CD806 (1:1000), anti-CD807 (1:1000), anti-CD808 (1:1000), anti-CD809 (1:1000), anti-CD810 (1:1000), anti-CD811 (1:1000), anti-CD812 (1:1000), anti-CD813 (1:1000), anti-CD814 (1:1000), anti-CD815 (1:1000), anti-CD816 (1:1000), anti-CD817 (1:1000), anti-CD818 (1:1000), anti-CD819 (1:1000), anti-CD820 (1:1000), anti-CD821 (1:1000), anti-CD822 (1:1000), anti-CD823 (1:1000), anti-CD824 (1:1000), anti-CD825 (1:1000), anti-CD826 (1:1000), anti-CD827 (1:1000), anti-CD828 (1:1000), anti-CD829 (1:1000), anti-CD830 (1:1000), anti-CD831 (1:1000), anti-CD832 (1:1000), anti-CD833 (1:1000), anti-CD834 (1:1000), anti-CD835 (1:1000), anti-CD836 (1:1000), anti-CD837 (1:1000), anti-CD838 (1:1000), anti-CD839 (1:1000), anti-CD840 (1:1000), anti-CD841 (1:1000), anti-CD842 (1:1000), anti-CD843 (1:1000), anti-CD844 (1:1000), anti-CD845 (1:1000), anti-CD846 (1:1000), anti-CD847 (1:1000), anti-CD848 (1:1000), anti-CD849 (1:1000), anti-CD850 (1:1000), anti-CD851 (1:1000), anti-CD852 (1:1000), anti-CD853 (1:1000), anti-CD854 (1:1000), anti-CD855 (1:1000), anti-CD856 (1:1000), anti-CD857 (1:1000), anti-CD858 (1:1000), anti-CD859 (1:1000), anti-CD860 (1:1000), anti-CD861 (1:1000), anti-CD862 (1:1000), anti-CD863 (1:1000), anti-CD864 (1:1000), anti-CD865 (1:1000), anti-CD866 (1:1000), anti-CD867 (1:1000), anti-CD868 (1:1000), anti-CD869 (1:1000), anti-CD870 (1:1000), anti-CD871 (1:1000), anti-CD872 (1:1000), anti-CD873 (1:1000), anti-CD874 (1:1000), anti-CD875 (1:1000), anti-CD876 (1:1000), anti-CD877 (1:1000), anti-CD878 (1:1000), anti-CD879 (1:1000), anti-CD880 (1:1000), anti-CD881 (1:1000), anti-CD882 (1:1000), anti-CD883 (1:1000), anti-CD884 (1:1000), anti-CD885 (1:1000), anti-CD886 (1:1000), anti-CD887 (1:1000), anti-CD888 (1:1000), anti-CD889 (1:1000), anti-CD890 (1:1000), anti-CD891 (1:1000), anti-CD892 (1:1000), anti-CD893 (1:1000), anti-CD894 (1:1000), anti-CD895 (1:1000), anti-CD896 (1:1000), anti-CD897 (1:1000), anti-CD898 (1:1000), anti-CD899 (1:1000), anti-CD900 (1:1000), anti-CD901 (1:1000), anti-CD902 (1:1000), anti-CD903 (1:1000), anti-CD904 (1:1000), anti-CD905 (1:1000), anti-CD906 (1:1000), anti-CD907 (1:1000), anti-CD908 (1:1000), anti-CD909 (1:1000), anti-CD910 (1:1000), anti-CD911 (1:1000), anti-CD912 (1:1000), anti-CD913 (1:1000), anti-CD914 (1:1000), anti-CD915 (1:1000), anti-CD916 (1:1000), anti-CD917 (1:1000), anti-CD918 (1:1000), anti-CD919 (1:1000), anti-CD920 (1:1000), anti-CD921 (1:1000), anti-CD922 (1:1000), anti-CD923 (1:1000), anti-CD924 (1:1000), anti-CD925 (1:1000), anti-CD926 (1:1000), anti-CD927 (1:1000), anti-CD928 (1:1000), anti-CD929 (1:1000), anti-CD930 (1:1000), anti-CD931 (1:1000), anti-CD932 (1:1000), anti-CD933 (1:1000), anti-CD934 (1:1000), anti-CD935 (1:1000), anti-CD936 (1:1000), anti-CD937 (1:1000), anti-CD938 (1:1000), anti-CD939 (1:1000), anti-CD